

Perturbative QCD predictions for two-photon exchange

Dmitry Borisyuk and Alexander Kobushkin
Bogolyubov Institute for Theoretical Physics
Metrologicheskaya street 14-B, 03680, Kiev, Ukraine

We study two-photon exchange (TPE) in the elastic electron-nucleon scattering at high Q^2 in the framework of pQCD. The obtained TPE amplitude is of order α/α_s with respect to Born approximation. Its shape and value are sensitive to the choice of nucleon wavefunction, thus study of TPE effects can provide important information about nucleon structure. With the wavefunctions based on QCD sum rules, TPE correction to the electron-proton cross section has negative sign, is almost linear in ε and grows logarithmically with Q^2 up to 7% at $Q^2 = 30 \text{ GeV}^2$. The results of existing "hadronic" calculations, taking into account just the nucleon intermediate state, can be smoothly connected with pQCD result near $Q^2 \sim 3 \text{ GeV}^2$. Above this point two methods disagree, which implies that "hadronic" approach becomes inadequate at high Q^2 . Other relevant observables, such as electron/positron cross section ratio, are also discussed.

I. INTRODUCTION

The two-photon exchange (TPE) in electron-proton scattering is actively discussed over last several years. The impetus for this was initially given by the discovery of so-called G_E/G_M problem in the proton form factor measurements [1]. It was shown later that the discrepancy between Rosenbluth separation and polarization transfer methods can be at least partially eliminated after taking into account TPE effects [2]. Several experiments aimed at direct detection of TPE contribution to cross section, are proposed [3]. Non-zero single-spin asymmetry, which is induced by the imaginary part of TPE amplitude, was observed experimentally [4]. The role of TPE in determination of proton radius [5], parity-violating observables [6] and in deep inelastic scattering [7] was also discussed.

Currently, the measurements of proton form factors at $Q^2 \sim 10 \text{ GeV}^2$ are in progress [8] and other measurements in this region are proposed [9, 10]. Clearly, these experiments call for the reliable estimate of TPE effects for high- Q^2 kinematics, which was one of the aims of the present work. At moderate Q^2 , the TPE amplitude was calculated using nucleon and resonances as intermediate states (further called "hadronic" approach) [2, 11, 12, 13]. At high Q^2 , however, a natural means for the description of any process involving hadrons, and in particular TPE, is perturbative quantum chromodynamics (pQCD). Surprisingly, we have found no direct pQCD calculation of TPE in the literature.

In Ref. [14], TPE at high Q^2 was investigated using the formalism of generalized parton distributions. The authors doubt of pQCD applicability in the presently accessible kinematical region and thus use an alternative method. The values of TPE corrections obtained this way have opposite sign to the results of "hadronic" calculations. The authors also use an assumption that the most important diagrams are that in which both photons interact with the same quark. It turns out that in pQCD approach the situation is reversed (see below, Sec. III B).

In the present paper we study TPE in the elastic electron-nucleon scattering at high Q^2 in the framework of pQCD. We employ the method, which was used to calculate baryon form factors in Refs. [15, 16]. In the adopted approach, a nucleon with momentum p is represented as three collinearly moving quarks with momenta $x_i p$, where $0 < x_i < 1$, $\sum_{i=1}^3 x_i = 1$. All quark masses and nucleon mass are neglected and thus $p^2 = (x_i p)^2 = 0$. The process amplitude has the form

$$\mathcal{M} = \langle \phi(y_i) | T(y_i, x_i) | \phi(x_i) \rangle \quad (1)$$

where T is hard scattering amplitude at quark level (represented by appropriate Feynman diagrams), $\phi(x_i)$ and $\phi(y_i)$ are initial and final nucleon spin-flavor-coordinate wavefunctions (quark distribution amplitudes). The convolution with nucleon wavefunction implies a convolution of spinor indices and an integration over $dx_1 dx_2 dx_3 \delta(1 - x_1 - x_2 - x_3)$ and similarly for y_i .

To obtain non-zero transition amplitude one must turn the momenta of all three quarks from initial to final direction. In one-photon exchange (Born) approximation one therefore needs at least two hard gluons to be exchanged between the quarks. It follows then that the amplitude scales as $\alpha \alpha_s^2 / Q^6$ and the nucleon form factor — as α_s^2 / Q^4 . In the case of TPE the exchange of one gluon is sufficient and thus the leading-order pQCD contribution to the TPE amplitude should be $\sim \alpha^2 \alpha_s / Q^6$. The ratio TPE/Born then will be not just α , as one may naively expect, but α/α_s , which is significantly larger and growing with Q^2 . Thus the larger Q^2 is, the more important TPE will be.

The paper is organized as follows. In Sec. II the observables, affected by TPE, are discussed, Sec. III describes all ingredients of calculation (hard scattering amplitude for one-photon and two-photon exchange and nucleon wavefunctions), numerical results are given in Sec. IV and conclusions — in Sec. V.

II. KINEMATICS AND OBSERVABLES

The momenta of particles are denoted according to $e(k) + N(p) \rightarrow e(k') + N(p')$. The transferred momentum is $q = p' - p$, $Q^2 = -q^2 > 0$ and $\nu = (p + k)(p' + k')$. The reduced cross section of elastic electron-proton scattering can be written as

$$\sigma_R = \frac{Q^2}{4M^2} |\mathcal{G}_M|^2 + \varepsilon |\mathcal{G}_E|^2 + \frac{Q^2}{4M^2} \frac{\varepsilon(1-\varepsilon)}{1+\varepsilon} |\mathcal{G}_3|^2 \quad (2)$$

where M is proton mass, $\varepsilon = 1 - 2[1 + \nu^2/Q^2(4M^2 + Q^2)]^{-1}$, which for $Q^2 \gg M^2$ turns to

$$\varepsilon \approx (\nu^2 - Q^4)/(\nu^2 + Q^4) \quad (3)$$

and \mathcal{G}_M , \mathcal{G}_E and \mathcal{G}_3 are certain invariant amplitudes (see details in Ref.[13]). In Born approximation \mathcal{G}_E and \mathcal{G}_M become usual electric and magnetic form factors and \mathcal{G}_3 vanishes, that is

$$\mathcal{G}_E = G_E + \delta\mathcal{G}_E, \quad \mathcal{G}_M = G_M + \delta\mathcal{G}_M, \quad \mathcal{G}_3 = \delta\mathcal{G}_3, \quad (4)$$

where the prefix δ indicates TPE contribution. The dominant part of the cross section at high Q^2 comes from the generalized magnetic form factor \mathcal{G}_M and can be written as

$$\sigma_R \approx \frac{Q^2}{4M^2} G_M^2 \left(1 + 2 \operatorname{Re} \frac{\delta\mathcal{G}_M}{G_M} \right) \quad (5)$$

Hence we should primarily study TPE contribution $\delta\mathcal{G}_M$. This quantity also defines the positron/electron elastic cross section ratio:

$$R = \frac{\sigma^+}{\sigma^-} = \left| \frac{G_M - \delta\mathcal{G}_M}{G_M + \delta\mathcal{G}_M} \right|^2 \approx 1 - 4 \operatorname{Re} \frac{\delta\mathcal{G}_M}{G_M} \quad (6)$$

The generalized electric form factor \mathcal{G}_E is suppressed in the cross section by $M^2/Q^2 \ll 1$. Therefore a consideration of TPE corrections to \mathcal{G}_E makes little sense.

The amplitude $\delta\mathcal{G}_3$ in principle can be measured in polarization experiments. Namely, neglecting terms of order M^2/Q^2 , the polarization of final proton in recoil polarization method is purely longitudinal and equals

$$P_\ell = h\sqrt{1-\varepsilon^2} \left(1 - \frac{2\varepsilon^2}{1+\varepsilon} \operatorname{Re} \frac{\delta\mathcal{G}_3}{G_M} \right) \quad (7)$$

where h is electron helicity. Thus a precise study of ε -dependence of P_ℓ may give an access to $\delta\mathcal{G}_3$.

III. AMPLITUDE CALCULATION

A. One-photon exchange

At first, we briefly review the pQCD calculation of form factors [15, 16]. The nucleon form factors, or the elastic electron-nucleon scattering in one-photon exchange approximation, is described in pQCD to leading order in α_s by 7 diagrams (Fig. 1a). For example, the piece of amplitude, coming from the first of them, is

$$\begin{aligned} \mathcal{M} = & -\frac{4\pi\alpha}{q^2} \left(\frac{4\pi\alpha_s}{q^2} \right)^2 \cdot 6 \cdot (4/9) \cdot (-q^2) \cdot \bar{u}'\gamma_\mu u \times \\ & \langle \phi(y_i) | e_1 \frac{\gamma_\alpha (y_1 \hat{p}' + y_2 \hat{p}' - x_2 \hat{p}) \gamma_\beta (x_1 \hat{p} + \hat{q}) \gamma_\mu \otimes \gamma_\alpha \otimes \gamma_\beta}{x_2^2 y_2 x_3 y_3 (y_1 + y_2) (1 - x_1) q^4} | \phi(x_i) \rangle \end{aligned} \quad (8)$$

where u and u' are electron spinors, the overall minus sign is due to *negative* electron charge, e_i is i th quark charge, $6 = 3!$ is a symmetry factor due to possible permutations of quark lines, $(-q^2)$ comes from quark and nucleon spinors normalization,

$$4/9 = \langle \frac{1}{2} \lambda^a \frac{1}{2} \lambda^b \otimes \frac{1}{2} \lambda^a \otimes \frac{1}{2} \lambda^b \rangle \quad (9)$$

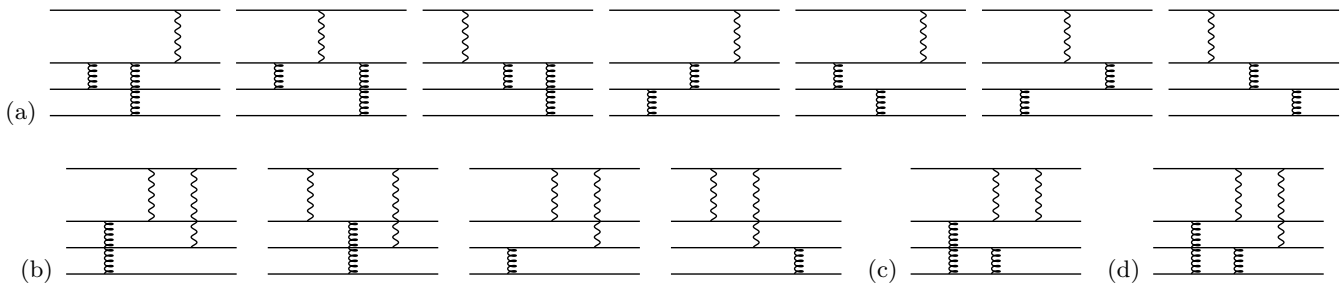


FIG. 1: pQCD diagrams for $eN \rightarrow eN$: one-photon exchange (a), two-photon exchange, leading order (b), subleading order (c,d).

is a color factor (here λ^a are Gell-Mann matrices and $\langle \rangle$ means averaging over totally antisymmetric color wavefunction). In the last equation as well as in Eq. (8) we separate matrices, acting on different quarks, by a \otimes sign. Thus in the expression for color factor $\frac{1}{2}\lambda^a\frac{1}{2}\lambda^b$ acts on the first, $\frac{1}{2}\lambda^a$ on the second and $\frac{1}{2}\lambda^b$ on the third quark.

Adding up contributions from all diagrams and using the fact that spin-flavor-coordinate wavefunction is totally symmetric under quark interchange, we obtain

$$\mathcal{M} = -\frac{4\pi\alpha}{q^2}\bar{u}'\gamma_\mu u \cdot \bar{U}'\gamma_\mu U \cdot G_M(q^2) \quad (10)$$

where U and U' are initial and final nucleon spinors and

$$G_M = \frac{16}{3} \left(\frac{4\pi\alpha_s}{q^2} \right)^2 \langle \phi(y_i) | (1 + h_1 h_3) \left\{ \frac{2e_1}{x_3 y_3 (1-x_1)^2 (1-y_1)^2} + \frac{2e_1}{x_2 y_2 (1-x_1)^2 (1-y_1)^2} + \frac{e_2}{x_1 y_1 x_3 y_3 (1-x_1)(1-y_3)} - \frac{e_1}{x_2 y_2 x_3 y_3 (1-x_1)(1-y_3)} - \frac{e_1}{x_2 y_2 x_3 y_3 (1-x_3)(1-y_1)} \right\} | \phi(x_i) \rangle \quad (11)$$

where $h_i = \pm 1$ are signs of quark helicities; the helicities of initial and final quarks should be equal. This is equivalent to well-known result [15, 16].

B. Two-photon exchange

For the case of TPE, there are only 4 distinct diagrams in the leading order (Fig. 1b), in which photons are connected to different quarks. The diagrams in which both photons interact with the same quark (Fig. 1c), need one more gluon to turn all quarks' momenta and thus are subleading in α_s . Moreover, the evaluation of such diagrams alone is inconsistent, since the contribution of the same order in α_s comes from one-gluon corrections to the leading diagrams (e.g. Fig. 1d).

One point needs to be clarified here. If we remove the electron line, the diagrams Fig. 1b-d will represent Compton scattering of virtual photons on the nucleon (doubly virtual Compton scattering, VVCS). And vice versa, TPE can be viewed as a process in which the virtual photon, emitted by the electron, is scattered from the proton and then absorbed back by the electron. VVCS has an important qualitative difference from the well-studied *real* Compton scattering (RCS). Since the momentum r of the real photon satisfies $r^2 = 0$, it cannot alone turn quark's momentum: $(x_i p - y_i p')^2 \neq 0 = r^2$. Therefore diagrams with the structure like (Fig. 1b) vanish for RCS, and the amplitude expansion begins with $O(\alpha_s^2)$ terms (diagrams like Fig. 1c,d). On contrary, VVCS photons may be highly virtual, diagrams Fig. 1b contribute, and leading terms in VVCS amplitude are $O(\alpha_s)$. Hence one cannot employ an analogy with RCS in the analysis of TPE (cf. Ref. [14]).

We write down the expression for the first diagram in Fig. 1b, the rest are analogous. We have

$$\delta\mathcal{M} = \left(\frac{4\pi\alpha}{q^2} \right)^2 \frac{4\pi\alpha_s}{q^2} \cdot 6 \cdot (-2/3) \cdot (-q^2) \times \langle \phi(y_i) | e_1 e_2 \frac{\bar{u}'\gamma_\mu(\hat{k} + x_2\hat{p} - y_2\hat{p}')\gamma_\nu u}{(k + x_2 p - y_2 p')^2 + i0} \cdot \frac{\gamma_\alpha(y_1\hat{p}' + y_3\hat{p}' - x_3\hat{p})\gamma_\mu \otimes \gamma_\nu \otimes \gamma_\alpha}{x_2 y_2 x_3^2 y_3 (x_1 + x_3)(y_1 + y_3)^2 q^2} | \phi(x_i) \rangle \quad (12)$$

where the color factor is $-2/3 = \langle \frac{1}{2}\lambda^a \otimes \frac{1}{2}\lambda^a \otimes 1 \rangle$. After some algebraic transformations and using wavefunction symmetry, we obtain the full TPE amplitude in the form

$$\delta\mathcal{M} = -\frac{4\pi\alpha}{q^2} \bar{u}'\gamma_\mu u \cdot \bar{U}'\gamma_\nu U \cdot \left(\frac{4p_\mu k_\nu}{\nu} \delta\mathcal{G}_3 + g_{\mu\nu} \delta G_M \right) \quad (13)$$

where

$$(\delta G_M, \delta\mathcal{G}_3) = -\frac{256\pi^2\alpha\alpha_s}{q^4} \langle \phi(y_i) | \frac{e_1 e_2 (1 - h_1 h_3)}{x_2 y_2 x_3 y_3 (1 - x_2)(1 - y_2)} \times \frac{1}{\nu(x_2 - y_2) - q^2(x_2 + y_2 - 2x_2 y_2) + i0} \left(\frac{\nu - q^2}{1 - x_2} + \frac{\nu + q^2}{1 - y_2} - 2\nu, 2\nu \right) | \phi(x_i) \rangle \quad (14)$$

From this expression it is easy to see the crossing symmetry of TPE amplitudes δG_M and $\delta\mathcal{G}_3$: both are ν -odd.

The quantity $\delta\mathcal{G}_M$, associated with the cross section correction (5), equals [13]

$$\delta\mathcal{G}_M = \delta G_M + \varepsilon \delta\mathcal{G}_3 \quad (15)$$

As implied by Eqs. (5-7), it is better to consider ratios $\delta\mathcal{G}_M/G_M$ and $\delta\mathcal{G}_3/G_M$ than the amplitudes themselves. This way we also avoid the uncertainty related with the absolute normalization of nucleon wavefunctions, since it cancels in the ratio. We have

$$\left(\frac{\delta G_M}{G_M}, \frac{\delta\mathcal{G}_3}{G_M} \right) = -\frac{3\alpha}{\alpha_s} \frac{\langle \phi(y_i) | (T_{\delta G_M}, T_{\delta\mathcal{G}_3}) | \phi(x_i) \rangle}{\langle \phi(y_i) | T_{G_M} | \phi(x_i) \rangle} \quad (16)$$

where T_{G_M} , $T_{\delta G_M}$ and $T_{\delta\mathcal{G}_3}$ are the expressions, sandwiched between wavefunctions in Eqs. (11,14).

The obtained TPE amplitudes are free from infra-red (IR) divergence. This becomes clear if we recall that the IR-divergent terms are proportional to Born amplitude. Thus $\delta\mathcal{G}_3$ is IR-finite (it vanishes in Born approximation), and

$$\delta G_M^{(\text{IR})} \sim \alpha G_M \ln \lambda^2 \quad (17)$$

where λ is infinitesimal photon mass. The magnetic form factor [Eq. (11)] is a quantity of order $O(\alpha_s^2)$. On the other hand, leading-order contribution to TPE is $O(\alpha_s)$ and therefore IR divergence should only appear as a *subleading* effect, in the next order in α_s .

Another interesting point pertains to photons' virtualities. In all diagrams they are both of order Q^2 , e.g. in the first diagram $q_1^2 = -x_2 y_2 Q^2$ and $q_2^2 = -(x_1 + x_3)(y_1 + y_3)Q^2$. We may conclude that the leading contribution to the amplitude at high Q^2 comes from the region where both photons are hard, $q_1^2 \sim q_2^2 \sim Q^2$.

C. Wavefunctions

Before turning to numerical calculations, we must specify a model for wavefunctions. The requirement for total spin and isospin to be 1/2 together with Pauli principle fix the following form of the quark distribution amplitude (for the proton of positive helicity):

$$|\phi(x_i)\rangle = \frac{f_N}{\sqrt{6}} \phi_1(x_1, x_2, x_3) (|u_\uparrow u_\downarrow d_\uparrow\rangle - |u_\uparrow d_\downarrow u_\uparrow\rangle) + \text{perm.} \quad (18)$$

where "perm." means sum over all quarks permutations and f_N is overall normalization constant not needed for our calculation. The neutron wavefunction is obtained by interchange $d \leftrightarrow u$. As we can see, the distribution amplitude is completely determined by the function ϕ_1 .

In general, the distribution amplitude and thus ϕ_1 depend logarithmically on Q^2 . Namely, we have

$$\phi_1(x_i, Q^2) = x_1 x_2 x_3 \sum_k [\alpha_s(Q^2)]^{\gamma_k} B_k P_k(x_1, x_3) \quad (19)$$

where P_k are Appell polynomials ($P_1 = 1$, $P_2 = x_1 - x_3$, etc.) and γ_k are corresponding anomalous dimensions [15]. Thus in the formal limit $Q^2 \rightarrow \infty$ the term with lowest γ_k , which is P_1 , dominates and $\phi_1 \rightarrow \phi_{as} = x_1 x_2 x_3$. This asymptotical wavefunction, however, leads to predictions inconsistent with experiment. In particular, it yields zero proton and positive neutron magnetic form factors. Thus at present Q^2 the distribution amplitude should be considerably different from its asymptotic form [16]. Since the evolution with Q^2 is very slow ($\gamma_k \ll 1$), the same wavefunction can be employed for all currently accessible Q^2 with a reasonable accuracy.

Various forms of distribution amplitude were proposed in the literature. We done the calculations with the following amplitudes: CZ [16], KS [17], COZ [18], GS [19] and Het [20]. The CZ and KS amplitudes give practically the same results as the COZ amplitude, thus they are not considered further.

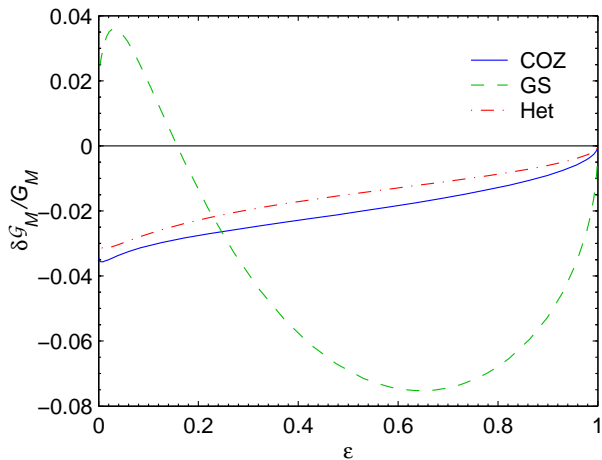


FIG. 2: TPE amplitude $\delta\mathcal{G}_M/G_M$ vs. ε at $Q^2 = 10$ GeV²

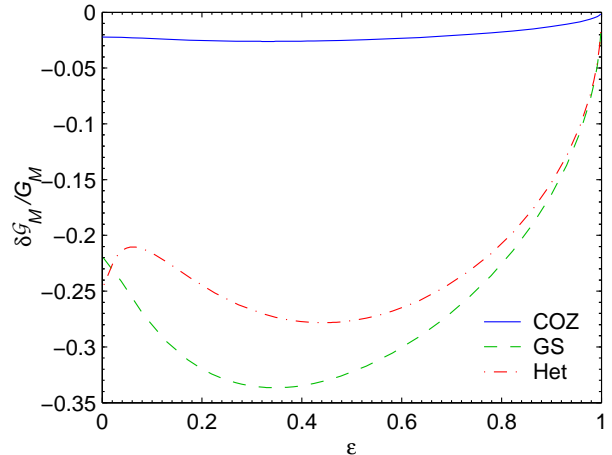


FIG. 3: TPE amplitude $\delta\mathcal{G}_M/G_M$ vs. ε for neutron at $Q^2 = 5$ GeV²

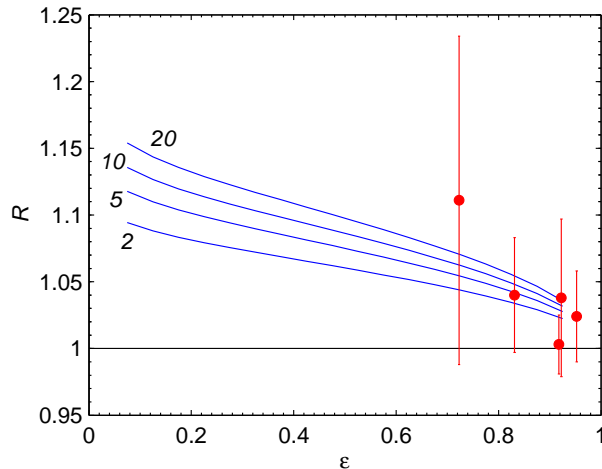


FIG. 4: Positron/electron cross section ratio for $Q^2 = 2, 5, 10$ and 20 GeV² (shown near the curves). Data are from Ref. [21] at $1.5 < Q^2 < 5$ GeV².

IV. NUMERICAL RESULTS

There are two independent kinematical variables in any elastic process. For eN scattering Q^2 and ε [Eq. (3)] are generally used. The ε -dependence of the obtained TPE amplitude $\delta\mathcal{G}_M$ is shown in Fig. 2. It turns out to be universal for all Q^2 (except for slow logarithmic evolution, which we neglect here). We see that the amplitude $\delta\mathcal{G}_M$, calculated with COZ and Het wavefunctions, is very close to the linear function of ε . Slight deviations from linearity are present near the endpoints $\varepsilon = 0$, $\varepsilon = 1$ only. In contrast, GS wavefunction yields much larger and highly nonlinear TPE amplitude. In light of this it is worth noting that linear ε -dependence of $\delta\mathcal{G}_M$ is necessary and sufficient for Rosenbluth plots to remain linear even under the influence of TPE [22]. Since careful analysis of experimental data do not reveal any nonlinearity in Rosenbluth plots [23], we conclude that the experiment disfavors GS wavefunction.

For the neutron target, both GS and Het wavefunctions yield nonlinear and anomalously huge TPE corrections, up to 25% (Fig. 3). Taking into account the smallness of neutron electric form factor, these corrections would manifest as severe nonlinearities of Rosenbluth plots, that is, strong ε -dependence of the elastic cross section. Though such cross section behaviour seems unlikely, the high- Q^2 neutron form factor data are too poor to draw a final conclusion. Further experimental study of electron-neutron elastic scattering at high Q^2 and different ε can show definitely whether the nucleon is described by Het or by COZ wavefunction. For the present moment we take the COZ wavefunction as the most plausible.

The amplitude $\delta\mathcal{G}_3$, which determines the correction to longitudinal recoil polarization [Eq. (7)], is small ($< 1\%$)

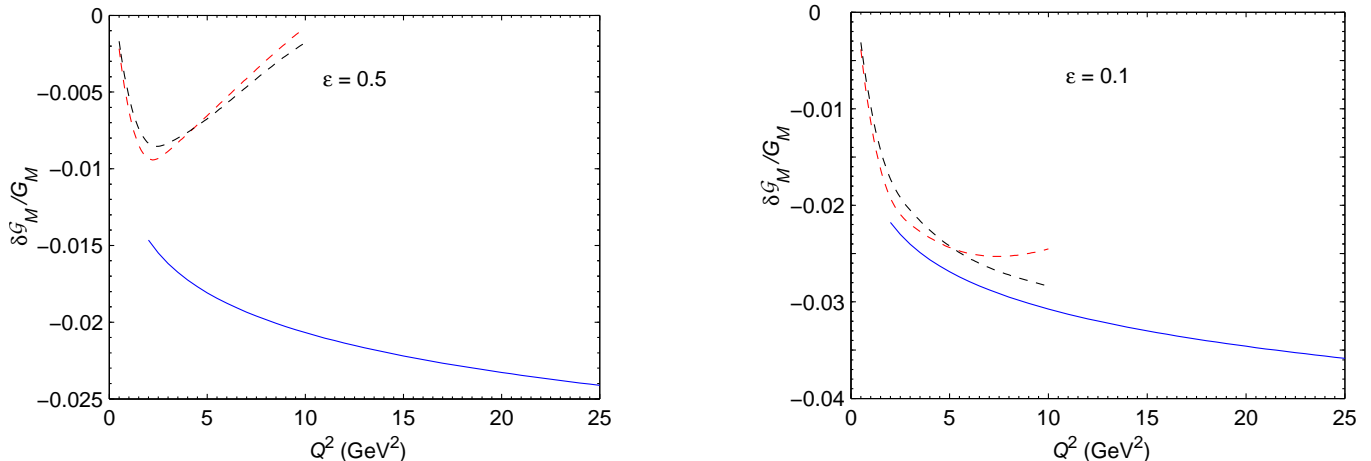


FIG. 5: TPE amplitude $\delta\mathcal{G}_M$ vs. Q^2 at $\varepsilon = 0.5$ (left) and $\varepsilon = 0.1$ (right). Dashed curves show hadronic calculations, with form factors parameterizations: dipole (red) and Ref. [24] (black).

for both proton and neutron, and unfortunately lies below the precision of today's experiments.

The positron/electron cross section ratio is shown in Fig. 4. The calculation is done with COZ wavefunction at $Q^2 = 2, 5, 10$ and 20 GeV^2 . The experimental data in the range $1.5 < Q^2 < 5 \text{ GeV}^2$ from Ref. [21] are also shown. Though the data points are well near the curves, the errors are very large. More precise data would be helpful, preferably in the low- ε region, where the predicted ratio is higher.

The Q^2 dependence of "normalized" TPE amplitudes at fixed ε is completely determined by evolution of strong coupling constant α_s . We have used simple parameterization

$$\alpha_s = \frac{4\pi}{\beta \ln(Q^2/\Lambda^2)} \quad (20)$$

with $\Lambda = 0.2 \text{ GeV}$. The resulting shape of TPE amplitude $\delta\mathcal{G}_M$ for proton, calculated with COZ wavefunction, is plotted in Fig. 5. At $Q^2 \approx 30 \text{ GeV}^2$, which is today the maximal Q^2 ever investigated, the relative value of TPE amplitude reaches 3.5%, which corresponds to cross section correction of about 7%. Such a correction is however smaller than the errors of available data. On the other hand, TPE can be seen in recently proposed high- Q^2 JLab experiment [9], where the estimated errors are at 1% level.

The results of "hadronic" calculation [11, 13] are also shown in Fig. 5 for comparison. Probably, the amplitude undergoes some gradual transition from this curve at lower Q^2 to pQCD prediction at higher Q^2 (recall that ε -dependence in both cases is the same, approximately linear with positive slope). The figure suggests that a reasonable interpolation is possible between the "hadronic" result for Q^2 below $\sim 3 \text{ GeV}^2$ and pQCD result above this value. But we also see a strong disagreement of these two curves at higher Q^2 . The most likely reason for such behaviour is that the "hadronic" approach, i.e. saturation of the intermediate hadronic states by the bare nucleon and the lowest resonances, is inadequate at high Q^2 . The multi-particle intermediate states yield a substantial part of the amplitude.

V. CONCLUSIONS

We have considered TPE for the elastic electron-nucleon scattering in the framework of pQCD. The calculations are done in the leading order with several model wavefunctions. For the proton target and wavefunctions based on QCD sum rules (CZ [16], KS [17] and COZ [18]), the TPE amplitude $\delta\mathcal{G}_M$, which determines cross section correction, has linear ε -dependence. Its value is of order α/α_s , grows logarithmically with Q^2 and at $Q^2 = 30 \text{ GeV}^2$ reaches 3.5% of Born amplitude. At lower Q^2 a smooth connection is possible with previous "hadronic" calculations, in which TPE amplitudes were calculated taking into account just the nucleon intermediate state [11]. On the other hand, at high Q^2 the results of these two methods are very different, which implies that "hadronic" approach becomes inadequate at $Q^2 \gtrsim 3 \text{ GeV}^2$.

The size and ε -dependence of TPE amplitudes are sensitive to the choice of nucleon wavefunction (quark distribution amplitude). At the same time, they are directly measurable: $\delta\mathcal{G}_M/G_M$ via cross section or positron/electron cross section ratio and $\delta\mathcal{G}_3/G_M$ — via longitudinal recoil polarization. Thus an accurate measurement of TPE observables opens a new efficient way to study quark distribution amplitude in the nucleon. For example, the existing

experimental data already rule out GS wavefunction (Ref. [19]). Since TPE amplitudes have non-trivial ε -dependence, they potentially provide much more information, than just nucleon form factors. Thus TPE turns from the correction to form factor measurements into an independent tool for studying nucleon structure.

Acknowledgments

This work was supported by Program of Fundamental Research of the Department of Physics and Astronomy of National Academy of Sciences of Ukraine.

-
- [1] J. Arrington, Phys. Rev. C **68**, 034325 (2003).
 - [2] P.G. Blunden, W. Melnitchouk and J.A. Tjon, Phys. Rev. C **72**, 034612 (2005).
 - [3] Measurement of the Two-Photon Exchange Contribution in ep Elastic Scattering Using Recoil Polarization (JLab experiment E04019), Spokespersons: R. Gilman, L. Pentchev, C. Perdrisat, R.Suleiman;
Beyond the Born Approximation: A Precise Comparison of Positron-Proton and Electron-Proton Elastic Scattering in CLAS (JLab experiment E04116), Spokespersons: A. Afanasev, J. Arrington, W. Brooks, K. Joo, B. Raue, L. Weinstein;
A Measurement of Two-Photon Exchange in Unpolarized Elastic Electron-Proton Scattering (JLab experiment E05017), Spokesperson: J. Arrington.
 - [4] S.P. Wells *et al.*, Phys. Rev. C **63**, 064001 (2001); F.E. Maas *et al.*, Phys. Rev. Lett. **94**, 082001 (2005).
 - [5] P.G. Blunden and I. Sick, Phys. Rev. C **72**, 057601 (2005).
 - [6] A.V. Afanasev and C.E. Carlson, Phys. Rev. Lett. **94**, 212301 (2005).
 - [7] A. Afanasev, M. Strikman and C. Weiss, Phys. Rev. D **77**, 014028 (2008).
 - [8] Measurement of G_{Ep}/G_{Mp} to $Q^2 = 9 \text{ GeV}^2$ via recoil polarization (JLab experiment E04108), Spokespersons: E. Brash, M. Jones, C. Perdrisat, V. Punjabi.
 - [9] Precision Measurement of the Proton Elastic Cross Section at High Q^2 (JLab experiment E1207108), Spokespersons: S. Gilad, B. Moffit, B. Wojtsekhowski, J. Arrington.
 - [10] Measurement of the Neutron Magnetic Form Factor at High Q^2 Using the Ratio Method on Deuterium (JLab experiment E1207104), Spokespersons: W.D. Brooks, G. Gilfoyle, K. Hafidi, M. Vineyard;
 - [11] D. Borisyuk and A. Kobushkin, Phys. Rev. C **74**, 065203 (2006).
 - [12] S. Kondratyuk and P.G. Blunden, Phys. Rev. C **75**, 038201 (2007).
 - [13] D. Borisyuk and A. Kobushkin, Phys. Rev. C **78**, 025208 (2008).
 - [14] A. Afanasev, S.J. Brodsky, C.E. Carlson, Y.C. Chen and M. Vanderhaeghen, Phys. Rev. D **72**, 013008 (2005).
 - [15] G.P. Lepage and S.J. Brodsky, Phys. Rev. D **22**, 2157 (1980). The expression for nucleon form factor in this paper has wrong overall sign.
 - [16] V.L. Chernyak and A.R. Zhitnitsky, Phys. Rep. **112**, 173 (1984).
 - [17] I.D. King and C.T. Sachrajda, Nucl. Phys. **B279**, 785 (1987).
 - [18] V.L. Chernyak, A.A. Ogloblin and I.R. Zhitnitsky, Yad. Fiz. **48**, 841 (1988).
 - [19] M. Gari and N.G. Stefanis, Phys. Rev. D **35**, 1074 (1987).
 - [20] N.G. Stefanis and M. Bergmann, Phys. Rev. D **47**, R3685 (1993).
 - [21] J. Mar *et al.*, Phys. Rev. Lett. **21**, 482 (1968).
 - [22] D. Borisyuk and A. Kobushkin, Phys. Rev. C **76**, 022201(R) (2007).
 - [23] V. Tvaskis *et al.*, Phys. Rev. C **73**, 025206 (2006).
 - [24] J.Arrington, W. Melnitchouk and J.A.Tjon, Phys. Rev. C **76**, 035205 (2007).